# Self-Assembly of Uniform Spherical Aggregates of Magnetic Nanoparticles through π–π Interactions**

Jian Jin, Tomokazu Iyoda, Changsheng Cao, Yanlin Song, Lei Jiang,* Tie Jin Li,* and Dao Ben Zhu

The assembly of nanostructured materials into organized and designed structures is an important goal in materials chemistry for application in electronic devices.[1] The building and patterning of inorganic nanoparticles into two- and three-dimensional organized structures by manipulation of individual units is a potential route to chemical, optical, magnetic, and electronic devices with useful properties.[2] Among these, the synthesis of magnetic nanoparticles which endow superparamagnetic properties is an issue of current interest, both from a fundamental point of view and for applications in materials science.[3–5] For example, the composite formed from magnetic nanoclusters and conducting oligomers may possess unique applications in such areas as electromagnetic interference shielding and electrochromic devices, as well as sensing and actuating technologies.[6, 7]

Self-assembly based on the spontaneous control of materials through noncovalent interactions (hydrogen bonding,[8, 9] van der Waals forces,[10, 11] and electrostatic forces[12, 13]) with no external intervention provides a powerful method for employing pre-programmed materials with the potential for multi-dimensional ordering for the creation of well-defined structure at a molecular level. Monolayer-functionalized nanoparticles that act as building blocks have been fabricated into ordered architectures for such approaches. Recently, Rotello and co-workers[14] reported that polymeric monolayer-protected gold particles self-assembled into spherical aggregates through hydrogen-bonding interactions. In their strategy, the polymers acted as the mortar to hold the colloidal particles together to form spherical aggregates. However, these aggregates were not very uniform, since the uniformity of the aggregates is governed by the uniformity of the polymer chain and the self-assembly process. Herein, we report the surprising finding that individual monolayer-coated magnetic nanoparticles self-assemble into uniform spherical aggregates through π–π interactions. The monolayer used was 2-carboxyterthiophene (TTP-COOH). Thiophene oligomers have been used as active organic semiconductor materials because of their attractive nature as conjugators and electrical conductors. Thiophene oligomers undergo self-assembly by holding together individual molecules (elemental bricks) in an orderly manner through weak van der Waals forces to build up materials.[15]

The formation of a magnetite crystal phase in a TTP-COOH-coated $Fe_3O_4$ aggregate powder was identified from the X-ray diffraction pattern (Figure 1). The pattern obtained confirms that the nanoparticles prepared in this study are the magnetite nanocrystals. The Bragg reflection peaks are all relatively broad because of the extremely small dimensions of the $Fe_3O_4$ nanocrystals.

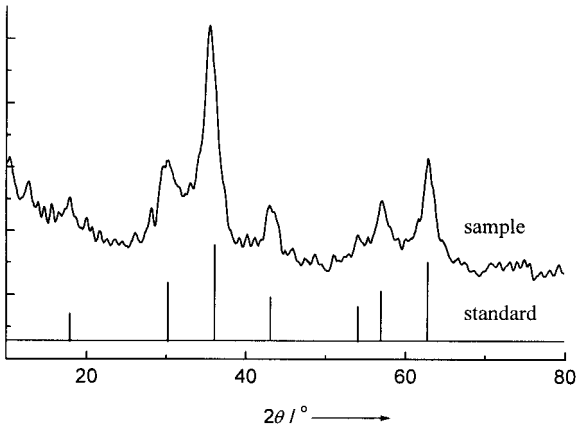


Figure 1. X-ray diffraction pattern of TTP-COOH-coated $Fe_3O_4$ aggregate powder. The vertical lines at the bottom are the reference data for the $Fe_3O_4$ standard taken from powder diffraction file 19-0629 from the Database of the International Center for Diffraction Data (ICDD).

The formation of self-assembled spherical aggregates can be directly visualized by transmission electron microscopy (TEM; Figure 2a, b). It can be seen that highly ordered and uniform spherical aggregates with a mean diameter of 148 ± 5 nm are obtained. These spherical aggregates are composed of 2000–4000 intensely dark spots per microsphere. These dark spots are individual TTP-COOH-coated $Fe_3O_4$ nanoparticles. Every nanoparticle, with a size of 6.0 ± 1.3 nm, appears as a discrete entity in the microsphere. The microspheres are transparent and the intersection between two clusters can be clearly seen. However, the interaction between individual particles is relatively weak and the spherical aggregates can be destroyed by sonication. As shown in Figure 2c, the self-assembled microspheres disappear after sonication treatment and the individual nanoparticles are monodispersed. The mean diameter of the individual nanoparticles is about 6–8 nm, which is consistent with the size of the dark spots in the microsphere.

A model for the self-assembly observed in the aggregated structure is shown in Figure 3. The driving force for the formation of aggregates is considered to be π–π interactions between individual nanoparticles. This can be confirmed by examination of the absorption spectra (Figure 4). Pure TTP-COOH in toluene shows one strong absorption band at 378 nm, while in TTP-COOH-coated $Fe_3O_4$ aggregates in

[*] Prof. L. Jiang, Dr. J. Jin, Y. Song, D. B. Zhu
Center of Molecular Sciences, Institute of Chemistry
Chinese Academy of Sciences
Beijing 100080 (PR China)
Fax: (+86) 10-82627566
E-mail: jianglei@infoc3.icas.ac.cn
Prof. T. J. Li, Dr. J. Jin, Dr. C. Cao
Department of Chemistry, Jilin University
Changchun 130023 (PR China)
Fax: (+86) 431-8923907
E-mail: tjli@mail.jlu.edu.cn
Prof. T. Iyoda
Department of Applied Chemistry, Faculty of Engineering
Tokyo Metropolitan University
1-1 Minami-Osawa Hachioji, Tokyo 192-03 (Japan)

[**] The authors thank the Special Research Foundation of the National Nature Science Foundation of China (29992530), State Key Project Fundamental Research (G1999064504) for continuing financial support.

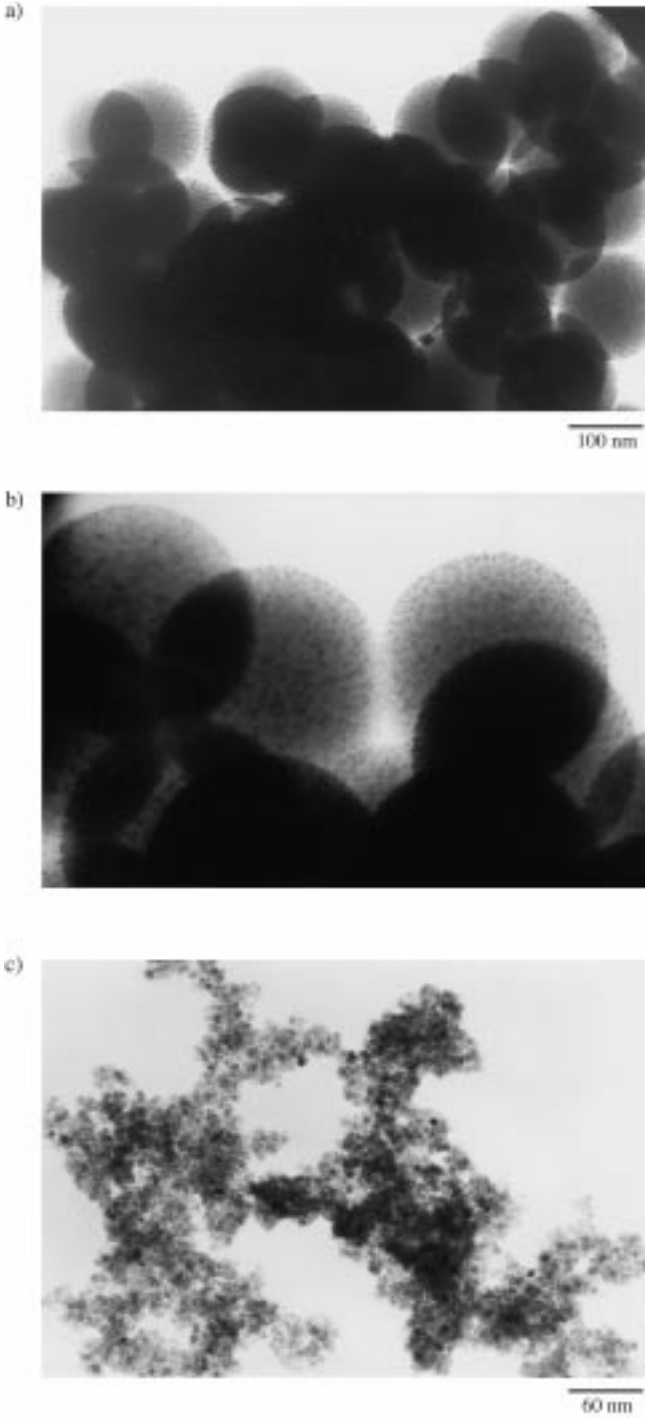


Figure 2. TEM images of a) self-assembled microspheres prepared by dropping the as-prepared TTP-COOH-coated $Fe_3O_4$ solution on a carbon-coated copper grid, b) enlarged image, c) parent solution treated by sonication (at a working frequency of 40 kHz for 20 min) dropped on a carbon-coated copper grid.

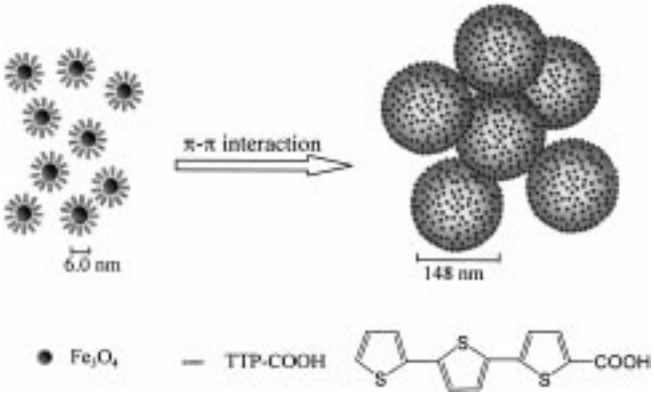


Figure 3. Structure model proposed for the self-assembly process of individual nanoparticles to form microspheres through $\pi-\pi$ interactions. The sizes of individual nanoparticles and microspheres can be determined directly by TEM.

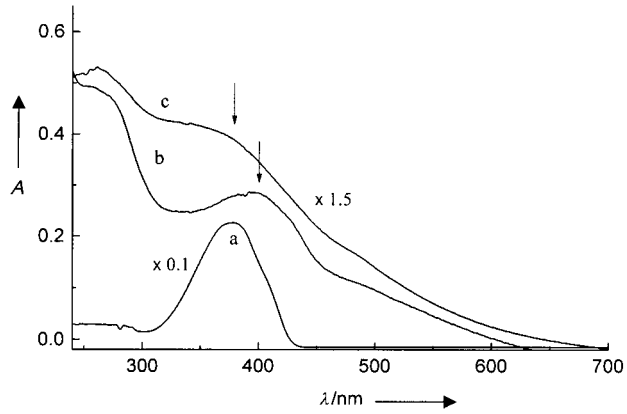


Figure 4. UV/Vis absorption spectra of a) pure TTP-COOH in toluene at a concentration of $5\times10^{-6}$ mol $L^{-1}$, b) as-prepared TTP-COOH-coated $Fe_3O_4$ solution in ethanol after dilution, and c) diluted TTP-COOH-coated $Fe_3O_4$ solution in ethanol after sonication (working frequency: 40 kHz).

ethanol the TTP-COOH absorption band is red-shifted to 400 nm. After sonicating the solution used to generate curve b, the red-shifted absorption band returns to 378 nm, which corresponds to the pure TTP-COOH absorption band. These results confirm the existence of $\pi-\pi$ interactions between individual nanoparticles in the microsphere. The anti-parallel dipole interaction between the conjugated backbone of terthiophene molecules in adjacent nanoparticles leads to the red-shift of the absorption band.[16] In general, there is an indirect dipole–dipole interaction between adjacent core/shell magnetic nanoparticles as a result of the existence of the shell.[17] The indirect magnetic interaction will cause the nanoparticles to form an isometric shape with a fractal structure.[18, 19] The formation of spherical aggregates in the present system indicates that the magnetic interaction contributes little to the structure compared with the effect of the $\pi-\pi$ interaction.

The formation of spherical aggregates from individual magnetic nanoparticles is considered to be a cooperative effect between the $\pi-\pi$ interaction and the particle growth in the given reaction environment. The formation of spherical aggregates is divided into two stages. The first stage is the formation of individual TTP-COOH-coated $Fe_3O_4$ nanoparticles. This is a rapid process and can be completed by vigorous stirring. The magnetite nanoparticles were synthesized by a typical chemical coprecipitation of $Fe^{II}$ and $Fe^{III}$ salts in ammonium hydroxide solution. The size of the nanoparticles is controlled by the reaction conditions, such as temperature, stirring rate, and concentration. In our experimental conditions, the size of the nanoparticles is

  1433-7851/01/4011-2136 $ 17.50+.50/0 *Angew. Chem. Int. Ed.* **2001**, *40*, No. 11

limited to 6–8 nm, which is in agreement with the results obtained by other researchers who used the same coprecipitation method.[20, 21] In the second stage, the individual nanoparticles coagulate into aggregates (called secondary particles) through intermolecular interactions ($\pi-\pi$ interactions), and is controlled by diffusion-controlled growth. According to the theory of diffusion-controlled growth, every nuclei gathers the neighboring primary particles within its individual field of attraction, which extends as a circular arc around a spherical particle to a defined distance from the center of the particle. It is not therefore surprising that the secondary particles obtained are spherical when the formation process is considered.[22] The growth of the microspheres in the water/oil (toluene) mixture solution is also influenced strongly by the variation of the surface energy with size. The particles tend to grow into a spherical shape in order to minimize their surface energy.[23] The critical size distribution of the spherical aggregates is also in accordance with the principle of diffusion-controlled growth, which states that the size distribution becomes narrower with particle growth.[24]

The magnetic characteristics of the aggregates were examined on a superconducting quantum interference device (SQUID) magnetometer. The field- and temperature-dependent magnetization data for the aggregates is shown in Figure 5. The curves obtained at 300 K are perfectly superimposable as the field is cycled between $-5$ and 5 kOe. The

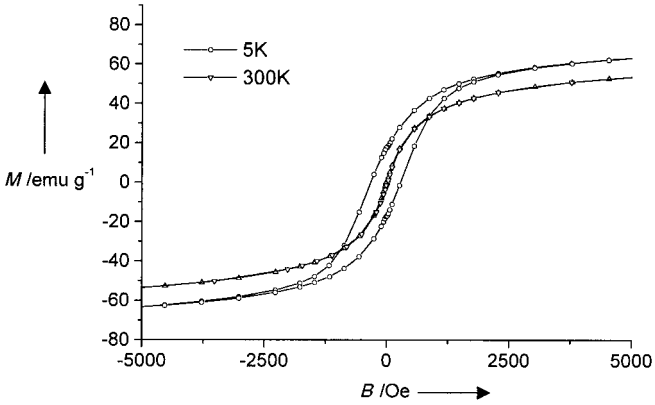


Figure 5. Magnetization versus applied field plots at 300 and 5 K for TTP-COOH-coated $Fe_3O_4$ aggregates.

curves are consistent with superparamagnetic behavior and the nanoscale dimensions of the particles.[25, 26] As the temperature is lowered to 5 K, the magnetization of the aggregates increases and exhibits a symmetric hysteresis loop, which indicates the transition from superparamagnetic to ferrimagnetic behavior.

In this work, a new method to build nanostructured spherical aggregates from individual magnetic nanoparticles has been developed. The results demonstrate a strategy directed by $\pi-\pi$ interactions for the self-assembly of individual magnetic nanoparticles into structured ensembles. Discrete microspheres formed using this method are highly ordered and uniform on the nanometer scale. This work represents a powerful and general strategy for the creation of highly structured multifunctional materials.

*Experimental Section*

Synthesis of 2-carboxyterthiophene: Terthiophene (2.480 g, 0.01 mol)[27] was added to dried THF (30 mL), and then a solution of lithium diisopropylamide ($LiN(iPr)_2$ 0.54 g, 5.0 mmol) in *n*-hexane (20 mL) added dropwise within 10 min. The reaction was maintained at $-87\,^{\circ}C$ for 1 h before purging with dried $CO_2$ gas for 30 min. The mixture was then stirred for 2 h at $-78\,^{\circ}C$. The temperature was then raised slowly to room temperature and stirred for 24 h. The resulting mixture was neutralized carefully by the addition of an aqueous solution of HCl (3%) and then filtered. Diethyl ether (100 mL) was added to the filtrate and the organic layer was washed sequentially with 3% aqueous HCl ($3\times10$ mL) and water ($3\times25$ mL). After drying with $MgSO_4$, the solvent was removed by rotary distillation. The resulting product was separated by column chromatography on $SiO_2$ ($4.0\times20$ cm, acetone/*n*-hexane 1/9). The product yield was 34.2%. M.p. 239–240 °C; FT-IR (KBr, $cm^{-1}$): $\tilde{\nu}=3066.26$, 1625.70, 1427.07, 696.18 (thiophene), 1625.70 (-CH=CH–CH=CH-), 1427.07 (=CH–S-), 1691.27 (-COOH); UV/Vis (DMF): 265, 378 nm. Elemental analysis calcd (%) for $C_{13}H_8O_2S_3$: C 54.87, H 3.28, S 31.39; found: C 54.83, H 3.19, S 31.07.

Synthesis of TTP-COOH-coated $Fe_3O_4$ nanoparticles and spherical aggregates: $FeCl_2\cdot4H_2O$ (0.15 g) and $FeCl_3\cdot6H_2O$ (0.416 g) were dissolved under $N_2$ in deaerated Milli-Q water (20 mL) with vigorous stirring. As the solution was heated to 60 °C, $NH_3\cdot H_2O$ (28% (w/w), 1 mL) was added, quickly followed by a solution of TTP-COOH (3 mg) in DMF (17 mL; a small quantity of toluene was added to enhance the solubility). The reaction was allowed to proceed for 1 h at 80 °C with constant and vigorous stirring to produce a stable, water-based suspension. The reaction mixture was then cooled slowly to room temperature. The suspension was washed sequentially with DMF, ethanol, and acetone (each $\times3$).

The X-ray diffraction pattern was recorded on a Rigaku D/max-2400 diffractometer using the monochromatized X-ray beam from nickel-filtered $Cu_{K\alpha}$ radiation. TEM was performed on a JEM 100CX electron microscope operating at 200 kV by placing a drop of the suspension solution onto a carbon-coated copper grid and letting the water evaporate slowly in air. The UV/Vis absorption spectra were recorded on a Shimadzu UV-3101 spectrophotometer. Magnetic data were obtained on a SQUID magnetometer (Quantum Design MPMS-5S).

Received: December 27, 2000 [Z16331]

[1] a) S. H. Sun, C. B. Murray, D. Weller, L. Folks, A. Moser, *Science* **2000**, *287*, 1989; b) A. P. Alivisatos, *Adv. Mater.* **1998**, *10*, 1297; c) T. L. Breen, J. Tien, S. R. J. Oliver, T. Hadzic, G. M. Whitesides, *Science* **1999**, *284*, 948; d) Y. Lu, H. Fan, A. Stump, T. L. Ward, T. Rieker, C. J. Brinker, *Nature* **1999**, *398*, 223.

[2] a) B. A. Korgel, D. Fitzmaurice, *Adv. Mater.* **1998**, *10*, 661; b) L. L. Beecroft, C. K. Ober, *Chem. Mater.* **1997**, *9*, 1302; c) C. B. Murray, C. R. Kagan, M. G. Bawendi, *Science* **1995**, *270*, 1335; d) C. A. Mirkin, R. L. Letsinger, R. C. Mucic, J. J. Storhoff, *Nature* **1996**, *382*, 607; e) O. Vidoni, K. Philippot, C. Amiens, B. Chaudret, O. Balmes, J. Malm, J. Bovin, F. Senocq, M. Casanove, *Angew. Chem.* **1999**, *111*, 3950; *Angew. Chem. Int. Ed.* **1999**, *38*, 3736.

[3] R. F. Ziolo, E. P. Giannelis, B. A. Weinstein, M. P. O'Horo, B. N. Ganguly, V. Mehrotra, M. W. Russell, D. R. Huffman, *Science* **1992**, *257*, 219.

[4] T. Prozorov, R. Prozorov, A. Gedanken, *Adv. Mater.* **1998**, *10*, 1529.

[5] C. Petit, A. Taleb, M. P. Pileni, *Adv. Mater.* **1998**, *10*, 259.

[6] B. Z. Tang, Y. Geng, J. W. Y. Lam, B. Li, X. Jing, X. Wang, F. Wang, A. B. Pakhomov, X. X. Zhang, *Chem. Mater.* **1999**, *11*, 1581.

[7] M. Kryszewski, J. K. Jeszka, *Synth. Met.* **1998**, *94*, 99.

[8] C. A. Mirkin, R. L. Letsinger, R. C. Mucic, J. J. Storhoff, *Nature* **1996**, *382*, 607.

[9] A. K. Boal, V. M. Rotello, *J. Am. Chem. Soc.* **2000**, *122*, 734.

[10] R. P. Andres, J. D. Bielefeld, J. I. Henderson, D. B. Janes, V. R. Kolagunta, C. P. Kubiak, W. J. Mahoney, R. G. Osifchin, *Science* **1996**, *273*, 1690.

[11] V. Patil, K. S. Mayya, S. D. Pradhan, M. Sastry, *J. Am. Chem. Soc.* **1997**, *119*, 9281.

[12] F. Caruso, A. S. Susha, M. Giersig, H. Möhwald, *Adv. Mater.* **1999**, *11*, 950.
[13] F. Caruso, R. Caruso, H. Möhwald, *Science* **1998**, *282*, 1111.
[14] A. K. Boal, F. Ilhan, J. E. Derouchey, T. Thurn-Albrecht, T. P. Russell, V. M. Rotello, *Nature* **2000**, *404*, 746.
[15] F. Garnier, A. Yassar, R. Hajlaoui, G. Horowitz, F. Deloffre, B. Servet, B. Ries, P. Alnot, *J. Am. Chem. Soc.* **1993**, *115*, 8716.
[16] E. G. Mcrae, M. Kasha, *J. Chem. Phys.* **1958**, *28*, 721.
[17] J. Dai, J. Q. Wang, C. Sangregorio, J. Fang, E. Carpenter, J. Tang, *J. Appl. Phys.* **2000**, *87*, 7397.
[18] M. P. Morales, S. Veintemillas-Verdaguer, M. I. Montero, C. J. Serrna, A. Roig, L. Casas, B. Martínez, F. Sandiumenge, *Chem. Mater.* **1999**, *11*, 3058.
[19] N. Moumen, P. Veillet, M. P. Pileni, *J. Magn. Magn. Mater.* **1995**, *149*, 67.
[20] L. Shen, P. E. Laibinis, T. A. Hatton, *Langmuir* **1999**, *15*, 447.
[21] L. Huo, W. Li, L. Lu, H. Cui, S. Xi, J. Wang, B. Zhao, Y. Shen, Z. Lu, *Chem. Mater.* **2000**, *12*, 790.
[22] T. Sugimoto, E. J. Matijevic, *J. Colloid Interface Sci.* **1980**, *74*, 227.
[23] X. Peng, J. Wickham, A. P. Alivisatos, *J. Am. Chem. Soc.* **1998**, *120*, 5343.
[24] The equation for diffusion-controlled growth is as follows: $\frac{dr}{dt} = DV_m\left(\frac{1}{r}+\frac{1}{\delta}\right)(C_b - C_e)$, where $r$ is the particle radius, $D$ is the diffusion coefficient, $V_m$ is the molar volume of the solid, $\delta$ is the thickness of the diffusion layer, $C_b$ is the bulk concentration of monomers, and $C_e$ is the solubility of the particle as a function of its radius. Here, $C_b - C_e$ can be regarded as constant, hence d$r$/d$t$ decreases with an increase in $r$. Related references: a) T. Sugimoto, *AIChE J.* **1978**, *24*, 1125; b) T. Sugimoto, *Adv. Colloid Interface Sci.* **1987**, *28*, 65.
[25] G. Bidan, O. Jarjayes, J. M. Fruchart, E. Hannecart, *Adv. Mater.* **1994**, *6*, 152.
[26] B. Z. Tang, Y. Geng, J. W. Y. Lam, B. Li, X. Jing, X. Wang, F. Wang, A. B. Pakhomov, X. X. Zhang, *Chem. Mater.* **1999**, *11*, 1581.
[27] M. Leclerc, K. Faid, *Adv. Mater.* **1997**, *9*, 1087.

## Dehydrogenative Dimerization of Tin Hydrides Catalyzed by Ruthenium – Allenylidene Complexes**

Susan M. Maddock and M. G. Finn*

The cycloaromatization rearrangement of *ortho* alkyl-substituted aromatic transition metal vinylidene complexes provides a means for a terminal alkyne to act as a synthon for a benzylic radical.[1] In an effort to engender the production of a higher-energy $sp^2$ radical, we have prepared several metal – allenylidene species with the requisite alkynyl substituents. In the course of screening H-atom donors with which to study the as yet undetermined decomposition pathways of these species, we observed a rapid dehydrogenative dimerization of tributyltin hydride, this dimerization requires the presence of a pendant unsaturated substituent. Here we describe this process and report the results of experiments designed to probe the catalytic mechanism.

The generation of $R_3Sn{-}SnR_3$ dimers from the corresponding monohydrides [Eq. (1)] is known to be catalyzed by a

$$R_3SnH \xrightarrow[\text{MeCN, EtCN, or } CH_2Cl_2]{\text{catalyst}} R_3Sn{-}SnR_3 + H_2 \qquad (1)$$

diverse set of transition metal complexes, including simple $Pd^{II}$ precursors,[2–4] $[Cp_2YH]$ (Cp = cyclopentadiene),[5] and $[(PPh_3)AuCl]$.[6] By far the most active catalysts are several diphosphane-bridged Fe/Pd heterobimetallic complexes in which the reaction is thought to occur at the Pd center, while the Fe center is proposed to play an important supporting role.[4, 7] Similar dehydrogenative pathways are presumably employed in the synthesis of oligomeric and polymeric diorganostannanes from tin dihydrides,[4] including reactions catalyzed by low-valent metallocene or Group VI hexacarbonyl complexes.[8]

Allenylidene complexes of the $[CpRu(PMe_3)_2]^+$ ion were prepared by the method of Selegue (details in Supporting Information).[9] A total of 13 derivatives were assembled (for the structures of complexes **1** – **13** see Table 1), in all cases, $^{13}C$ NMR signals were observed at $\delta = 293-299$, 213 – 228, and 149 – 154, for the $C_\alpha$, $C_\beta$, and $C_\gamma$ centers, respectively, with no attached protons, and a sharp band was found in the infrared spectrum at 1913 – 1925 $cm^{-1}$. These data serve to substantiate the allenylidene structure and rule out the cyclic isomer recently identified for analogous complexes of the $[Cl_2(PR_3)_2Ru]$ fragment.[10] An X-ray crystal structure obtained for the *para*-nitro derivative **12** (Supporting Information)[11] is similar to the parent complex **2**.[12]

Complex **1** (see Table 1), prepared for the study of diradical cycloaromatization, induces rapid gas evolution and clean production of $(Bu_3Sn)_2$ when added to a large excess of $Bu_3SnH$ in acetonitrile or dichloromethane. With 3 mol% **1** relative to tin hydride, 96% conversion is obtained within 10 mins at room temperature under nitrogen atmosphere. The structural elements necessary for catalysis were probed with complexes **2** – **12** (Table 1).[13] Comparisons of activity were made by determining the extent of conversion of $Bu_3SnH$ after exactly 5 mins under a standard set of conditions (1.4 mol% ruthenium catalyst relative to $Bu_3SnH$); such results do not allow separate analysis of the initial rate and lifetime. Of those species bearing substituents in the *ortho* position, allenylidenes **3** and **4** are of comparable activity to **1** (Table 1), demonstrating that the olefinic moiety of **1** (intended as an intramolecular radical trap in the event of cycloaromatization) is not involved in the catalytic process. Vinylidene complexes **14** and **15**, analogous to **4**, and the

[*] Prof. M. G. Finn, Dr. S. M. Maddock
Department of Chemistry
The Scripps Research Institute
10550 North Torrey Pines Rd., La Jolla, CA 92037 (USA)
Fax: (+1) 858-784-8850
E-mail: mgfinn@scripps.edu

[**] We thank The Skaggs Institute for Chemical Biology at The Scripps Research Institute for support of this work; S.M.M. is a Skaggs Postdoctoral Fellow. We are also grateful to Dr. Michal Sabat (University of Virginia) for X-ray crystallography and Prof. David Goodin (The Scripps Research Institute) for the EPR experiment described in ref. [14].

Supporting information for this article is available on the WWW under http://www.angewandte.com or from the author.

  1433-7851/01/4011-2138 $ 17.50+.50/0 